Proceedings of the 21st ICSMGE, Vienna, Austria, 14 – 19 June 2026. Pistrol, Adam & Schweiger (eds.)
Published by: ÖGG, Austrian Society for Geomechanics, Salzburg, Austria, ISBN 978-3-9503898-4-5
https://doi.org/10.53243/ICSMGE2026-1312

Modelling of fully saturated freezing soils

Haitao Jing, Wenjie Cui, Xiaotian Wu
School of Transportation Science and Engineering, Beihang University, Beijing, hjing@buaa.edu.cn

David M. Potts, Lidija Zdravkovic
Imperial College London, London, UK

ABSTRACT: The mechanical behaviour of seasonal freezing soils is primarily controlled by temperature variations and the associated ice content in the soils pores. To capture the thermo-mechanical feature of fully saturated freezing soils, a constitutive model is proposed in this paper within the framework of double stress variables. This model employs improved expressions for both the yield surface and the plastic potential which allow the selection of flexible shapes. A novel formulation is introduced to adequately model the temperature-dependent variation of elastic bulk and shear moduli for freezing soils, which overcomes the limitation in existing models that the elastic moduli cannot reduce to those for a conventional critical state model when the temperature exceeds the freezing point. The proposed constitutive model has been implemented into the bespoke finite element code employed in this research, and its features are demonstrated through a series of numerical simulations under various stress paths. Finally, the performance of the model is verified against existing experimental results for fully saturated freezing soils, yielding a good agreement.

KEYWORDS: Freezing soils, constitutive relation, finite element method, temperature variation, elastic moduli.

1 INTRODUCTION

The deformation of seasonal freezing soils due to temperature variations, including frost heave and thaw settlement, can impose significant challenges to geotechnical engineering designs. To date, numerous constitutive models have been proposed to capture the complex mechanical behaviour of seasonal freezing soils (e.g. Nixon, 1991; Nicolsky et al., 2008).

Thermo-elastic models have been firstly adopted in the analysis of seasonal freezing soils (e.g. Li et al., 2008; Thomas et al., 2009). However, the irreversible volumetric change induced by cyclic temperature change is neglected. To capture the complex temperature dependent constitutive behaviour of freezing soils under various stress paths, many thermo-elasto-plastic models have been developed. These models, mainly developed for fully saturated freezing soils, can generally be classified based on the number of the adopted stress variables. He et al. (2000) presented a visco-elasto-plastic damage model based on the generalised Mises failure criterion to describe the damage behaviour of frozen soils. Arenson & Springman (2005) proposed an elasto-plastic model incorporating the Mohr-Coulomb failure criterion to capture the creep behaviour of ice-rich frozen soils. Lai et al. (2014) developed a constitutive model by employing the hyperplasticity theory to characterise the mechanical behaviour of frozen loess. In the above models, a single stress variable, i.e., the total stress, is adopted to derive the stress-strain relationship of fully saturated freezing soils and the influence of confining pressure is emphasised in the associated modelling. However, this type of model, as pointed out by Ghoreishian Amiri et al. (2016), cannot adequately account for the deformation induced by temperature changes for fully saturated freezing soils.

To overcome the limitations of single stress variable models, the first double stress variables model was developed by Nishimura et al. (2009), based on the framework of the Barcelona Basic Model (BBM), in which the net stress and cryogenic suction were employed as two independent stress variables. The net stress is defined as the difference between the total stress and the pore ice pressure, while the cryogenic suction refers to the surface tension at the ice-water interface, defined as the difference between the pore ice pressure and the pore fluid pressure. To account for the contribution of pore ice to shear resistance, an alternative definition of the solid phase stress, instead of the net stress, was introduced by Ghoreishian Amiri et al. (2016), with which a constitutive model for fully saturated freezing soils was developed and subsequently applied in the finite element (FE) modelling of Caen frost heave experiments undertaken in a large-scale laboratory facility in Caen, France (Rostami et al., 2017).

This paper proposes a constitutive model for fully saturated freezing soils within the framework of double stress variables. Improved expressions proposed by Lagioia et al. (1996) are employed for both yield surface and the plastic potential, which allow the selection of flexible shapes. A novel formulation is introduced to adequately model the temperature-dependent variation of elastic bulk and shear moduli for fully saturated freezing soils enabling the proposed model to reduce to a conventional critical state model when the temperature exceeds the freezing point. The proposed constitutive model has been implemented into the bespoke FE software ICFEP (Imperial College Finite Element Program, Potts & Zdravković, 1999, 2001) which was employed to perform all analyses presented in this paper. A compression positive sign convention is adopted for the presented formulations and simulation results.

2 MODEL FORMULATION

2.1 *Stress variables and strain components*

Due to the observed similarities in phase composition, stress state, and characteristic curves between fully saturated freezing soils and partially saturated soils (Black & Tice, 1989), the framework of double stress variables presented by Alonso et al. (1990) and Georgiadis et al. (2005) is employed in this study. For fully saturated freezing soils, the solid phase stress $\{\sigma^*\}$ and the cryogenic suction s_{eqi} are adopted as the two dependent stress variables. The solid phase stress $\{\sigma^*\}$, representing the stress carried by soil particles and ice, is defined as:

$$\{\sigma^*\} = \{\sigma\} - s_l\{\sigma_f\} \tag{1}$$

where $\{\sigma\}$ is the total stress, $\{\sigma_f\} = \{p_f \quad p_f \quad p_f \quad 0 \quad 0 \quad 0\}^T$, p_f is the pore fluid pressure and s_l is the degree of liquid ice saturation which can be defined using a Van Genuchten type of expression as:

$$s_l = \left\{1 + \left[\alpha\left(T_{entry} - T\right)\right]^n\right\}^{-m} \bullet (1 - s_{l0}) + s_{l0} \tag{2}$$

where s_{l0} is the degree of liquid ice saturation in the long term, T is the temperature, T_{entry} refers to the freezing point, α, n and m are fitting parameters. Cryogenic suction s_{eqi} corresponds to

the surface tension at the ice-water interface and is derived from the Clausius-Clapeyron equation as (Nishimura et al., 2009):

$$s_{eqi} = -\rho_i L_i ln\left(\frac{T - T_{ref}}{T_{entry} - T_{ref}}\right) \tag{3}$$

where ρ_i is the ice density, L_i is the specific latent heat of fusion and T_{ref} is a reference temperature. When the temperature exceeds the freezing point, $s_l = 1$, the solid phase stress $\{\sigma^*\}$ reduces to the effective stress and $s_{eqi} = 0$. Consequently, the framework of double stress variables reduces to that of a single stress variable (i.e. effective stress), which is consistent with a conventional critical state model for fully saturated soils.

Following a similar approach for partially saturated soils, the incremental total strain $\{d\varepsilon\}$ can be written as:

$$\{d\varepsilon\} = \{d\varepsilon_m^e\} + \{d\varepsilon_m^p\} + \{d\varepsilon_s^e\} + \{d\varepsilon_s^p\} \tag{4}$$

where $\{d\varepsilon_m^e\}$ and $\{d\varepsilon_m^p\}$ represent the incremental elastic and plastic strains associated with the solid phase stress respectively, while $\{d\varepsilon_s^e\}$ and $\{d\varepsilon_s^p\}$ represent the incremental elastic and plastic strains due to the change in the cryogenic suction respectively.

2.2 *Elastic strains*

The incremental elastic strain associated with the solid phase stress can be defined as:

$$d\varepsilon_v^{me} = dp^*/K \tag{5}$$

$$dE_d^{me} = dJ^*/G \tag{6}$$

where $d\varepsilon_v^{me}$ and dE_d^{me} represent the incremental elastic volumetric and deviatoric strains induced by the change in solid phase stress respectively, dp^* and dJ^* are the incremental mean and deviatoric solid phase stresses respectively, and K and G are the elastic bulk and shear moduli respectively.

The elastic bulk modulus K is observed to vary with the ice content in the pore and hence is expressed as:

$$K = s_l K_{uf} + (1 - s_l)K_{ff} \tag{7}$$

$$K_{uf} = vp^*/\kappa_0 \tag{8}$$

$$K_{ff} = \left\{\left[m_{K_f}\left(T_{entry} - T\right)\right]^{n_{K_f}} + 1\right\} vp^*/\kappa_0 \tag{9}$$

where v is the specific volume, κ_0 is the slope of the swelling line for unfrozen soils in the $v - lnp^*$ plane, and m_{K_f} and n_{K_f} are fitting parameters. The variation of K with different values of fitting parameters, is shown in Figure 1. It is noted that when the temperature exceeds the freezing point, K reduces to K_{uf}, which is consistent with a conventional critical state constitutive model. This formulation overcomes the deficiency of some existing constitutive models that fail to reduce to a conventional critical state model when the soil becomes unfrozen (Ghoreishian Amiri et al., 2016).

The elastic shear modulus G is formulated in a similar manner and is given as:

$$G = s_l G_0 + (1 - s_l)G_f \tag{10}$$

$$G_f = G_{f_{ref}} - G_{f_{inc}} \bullet \left(T - T_{E,ref}\right) \tag{11}$$

where, G_0 and G_f are the elastic shear moduli of the soils under unfrozen and fully frozen states, respectively, $G_{f_{ref}}$ is a reference value of G_f at the reference temperature of $T_{E,ref}$ and $G_{f_{inc}}$ is the associated rate of change with respect to temperature.

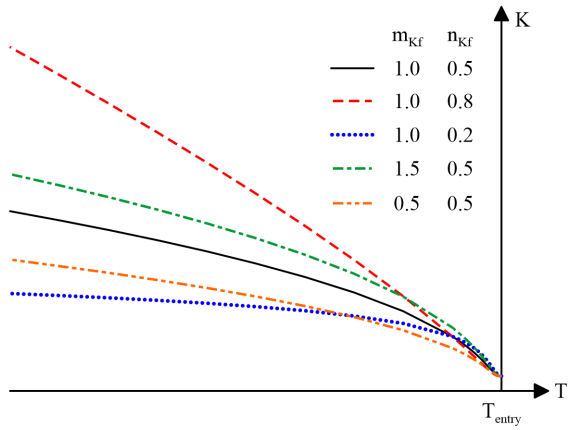

Figure 1. Variation of the elastic bulk modulus K with temperature.

The incremental elastic strain associated with the cryogenic suction is given following a consistent form to that associated with the matric suction in the BBM (Alonso et al., 1990):

$$d\varepsilon_s^e = \frac{\kappa_s}{3v\left(s_{eqi} + p_{atm}\right)} ds_{eqi} \tag{12}$$

where κ_s is the elastic compression coefficient for changes in cryogenic suction and p_{atm} is the atmospheric pressure.

2.3 *Yield function and Plastic potential*

To enable flexible shapes for both the primary yield surface and its plastic potential, the improved expression proposed by Lagioia et al. (1996) is adopted:

$$F_1 = G_1 = \frac{p^* + ks_{eqi}}{p_0 + ks_{eqi}} - \frac{\left(1 + \frac{\eta_i}{K_{2i}}\right)^{\frac{K_{2i}}{\beta_i}}}{\left(1 + \frac{\eta_i}{K_{1i}}\right)^{\frac{K_{1i}}{\beta_i}}} \tag{13}$$

where, F_1 and G_1 refer to the primary yield surface and plastic potential, respectively, k is a parameter governing the increase in apparent cohesion induced by cryogenic suction, p_0 is the hardening parameter, K_{1i}, K_{2i} and β_i are constants controlling the shape of the surface which depends on model parameters α_i and μ_i, $\eta_i = \sqrt{J_{2\eta}/J_{2\eta i}}$ is the generalised normalised stress ratio, $J_{2\eta} = \left[J^*/(p^* + ks_{eqi})\right]^2$ is the square of the stress ratio, $J_{2\eta i}$ is the value of $J_{2\eta}$ when failure is reached, and the subscripts $i = f, g$ denote the yield surface and plastic potential, respectively. Further details of this expression can be found in Lagioia et al. (1996).

The primary isotropic yield limit is expressed as:

$$p_0 = p^c \left(\frac{p_0^*}{p^c}\right)^{\frac{\lambda(0)-\kappa}{\lambda(s)-\kappa}} \tag{14}$$

where p_0^* is the hardening parameter in the unfrozen state, p^c is a reference stress, $\lambda(s)$ and $\kappa = vp^*/K$ are the slopes of the normal compression and swelling lines in the $v - lnp^*$ plane, respectively, with $\lambda(s)$ being expressed as:

$$\lambda(s) = \lambda(0)\left[(1 - r)e^{-\beta s_{eqi}} + r\right] \tag{15}$$

where $\lambda(0)$ is the value of $\lambda(s)$ at $s_{eqi} = 0$, and r and β are fitting parameters.

The secondary isotropic yield surface F_2 and its associated plastic potential G_2 are also adopted in a form consistent with the framework of the BBM:

$$F_2 = G_2 = s_{eqi} - s_{oi} \tag{16}$$

where s_{oi} is the initial hardening parameter for the secondary isotropic yield surface. A schematic diagram of the complete yield surfaces is shown in Figure 2.

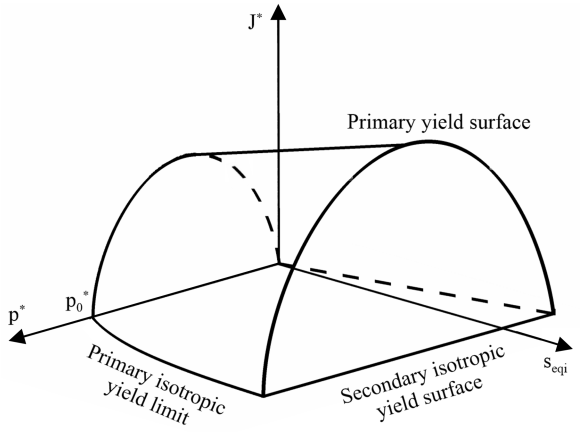

Figure 2. Schematic diagram of the complete yield surfaces.

2.4 *Hardening rules*

The incremental plastic volumetric strains associated with the cryogenic suction and the solid phase stress, i.e. $d\varepsilon_v^{sp}$ and $d\varepsilon_v^{mp}$ are assumed to exert comparable influences on the hardening parameter p_0^*. Therefore, the hardening rule for the primary yield surface can be expressed as:

$$\frac{dp_0^*}{p_0^*} = \frac{v}{\lambda(0)-\kappa_0}\left(d\varepsilon_v^{mp} + d\varepsilon_v^{sp}\right) \tag{17}$$

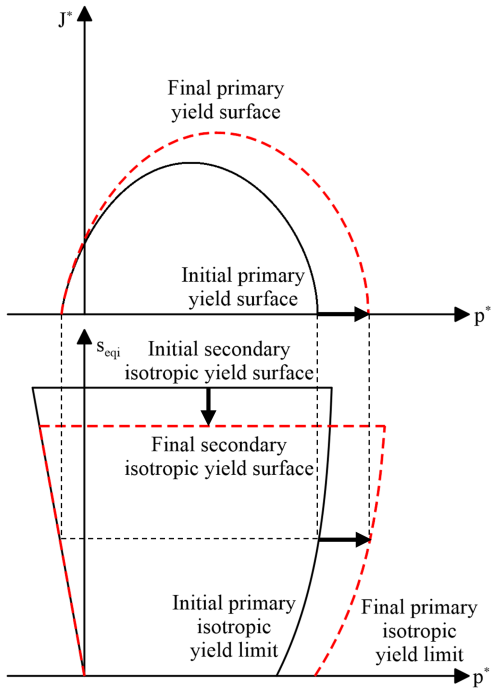

Figure 3. Coupling between primary and secondary isotropic yield surfaces.

A similar assumption is adopted for the secondary isotropic yield surface, and the corresponding hardening rule is derived as:

$$\frac{ds_{oi}}{s_{oi}+p_{atm}} = -\frac{v}{\lambda_s+\kappa_s}\left[\frac{1}{s_l}d\varepsilon_v^{sp} + \left(1-\frac{s_{eqi}}{s_{oi}}\right)d\varepsilon_v^{mp}\right] \tag{18}$$

where λ_s is the compression coefficient for changes in cryogenic suction. Equations (17) and (18) imply that the two yield surfaces are coupled. Activation and movement of either of the two surfaces will cause movement of the other (as shown in Figure 3).

3 MODEL PERFORMANCE

As the constitutive model proposed in this paper is formulated within the framework of double stress variables, its feature under triaxial loading paths is similar to that of existing constitutive models for partially saturated soils, e.g. BBM and Imperial College Single Structure Model (ICSSM) proposed by Georgiadis et al. (2005), and therefore is not discussed in this paper. The performance of the proposed model under the stress path of thermal loading (i.e. freezing-thawing) is the main focus of this section.

3.1 *Freezing-thawing for heavily overconsolidated soils*

A typical freezing stress path for heavily overconsolidated soils is firstly employed. As shown in Figure 4, the initial stress point A locates within both the initial primary and secondary isotropic yield surfaces. When the temperature decreases, the cryogenic suction s_{eqi} increases and the solid phase stress p^* rapidly increases before the secondary yield limit is reached (point B). Further decreasing the temperature leads to an increase in the size of the secondary yield surface and a reduction in the size of the primary yield limit, while p^* tends to stabilise. This model feature depends on the definition of solid phase stress expressed by Equation (1). During freezing, the total stress remains constant, while s_l initially rapidly decreases based on Equation (2), resulting in a significant increase in p^*. When the temperature is sufficiently low, s_l becomes stable and hence p^* remains almost constant.

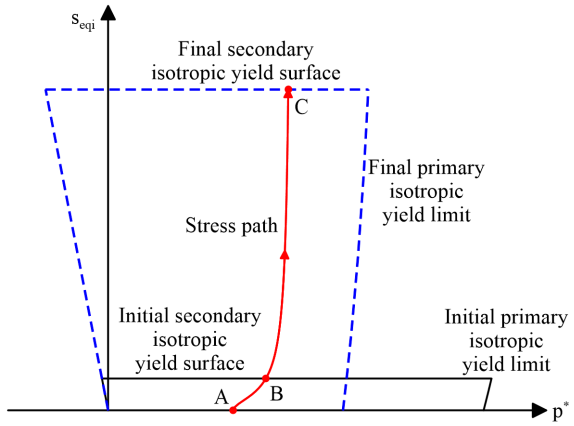

Figure 4. Stress path of freezing for heavily overconsolidated soils.

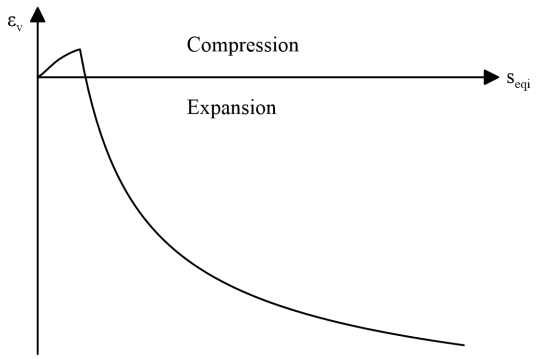

Figure 5. Variation of accumulated total strain during freezing.

Figure 5 shows the associated accumulated total volumetric strain ε_v during freezing. An initial compressive volumetric change of the soil is firstly observed, followed by a rapid

volume expansion. This response is associated with the hardening laws and the evolution of the yield surfaces. The initial stress point A is located inside the yield surfaces. A reduction in temperature results in elastic volumetric compression induced by the increases in s_{eqi} and p^*, as shown in Equations (5) and (12). When the stress point reaches the secondary isotropic yield surface (point B), further freezing leads to the activation of the associated hardening laws shown by Equation (18), resulting in dilative volumetric changes. It should be noted that at this stage, the magnitude of the elastic volumetric compression is significantly lower than that of the plastic volumetric expansion, resulting in an expansion in the total volume of the soil.

The stress path of thawing for heavily overconsolidated soils is shown in Figure 6. The initial stress point A is within the yield surfaces. With increasing temperature, p^* remains approximately constant initially before exhibiting a gradual decrease when the freezing point is approached, which is consistent with the variation of s_l. During the thawing process, only compressive elastic volumetric change due to decreases in s_{eqi} and p^* occurs.

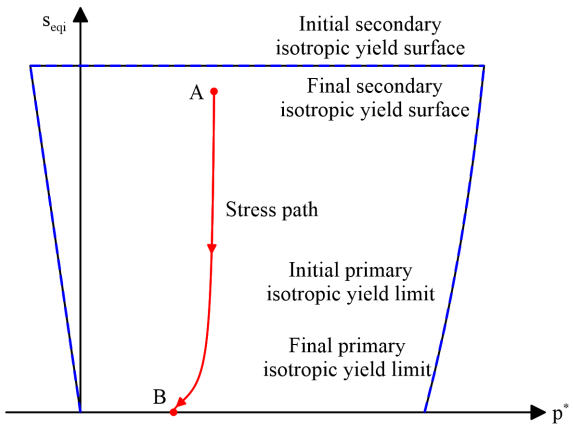

Figure 6. Stress path of thawing for heavily overconsolidated soils.

3.2 *Freezing-thawing for normally consolidated soils*

Figure 7 shows the stress path of freezing for normally consolidated soils. During the initial freezing stage, the stress point A locates on the primary isotropic yield limit. Decreasing the temperature results in compressive plastic volumetric strain due to the activation of primary isotropic yielding, while the position of the secondary isotropic yield surface moves downwards. When the secondary isotropic yield surface is reached, the stress point (i.e. point B) actually locates at the intersection of two yield surfaces. Further decreasing the temperature leads to the increase in both the cryogenic suction s_{eqi} and the solid phase stress p^* , and the stress point tends to move toward the upper right direction, indicating that both the primary and secondary isotropic yielding will be simultaneously active. Details of the relevant formulation and algorithm when two yield surfaces are simultaneously active can be found in Potts & Zdravković (1999). In contrast, for partially saturated soil models such as BBM or ICSSM, the model stress (i.e. net stress) will stay unchanged with increasing/decreasing suction. Therefore, the stress point will move vertically instead of toward the upper right direction. If the stress points locates at the intersection of the two yield surfaces, only one yield surface will be active during drying/wetting.

The stress path of thawing for normally consolidated soils is shown in Figure 8. The stress point A initially locates on the primary isotropic yield limit. At the beginning of the thawing process, a slight decrease in s_{eqi} activates the primary isotropic yielding, resulting in plastic volumetric expansion of the soil. The primary isotropic yield limit moves rightward, while the secondary isotropic yield surface moves downward. Consequently, further decrease in p^* leads to the detachment of the stress point from the primary isotropic yield limit. The stress state subsequently becomes purely elastic and the associated model feature is similar to that shown in Figure 6.

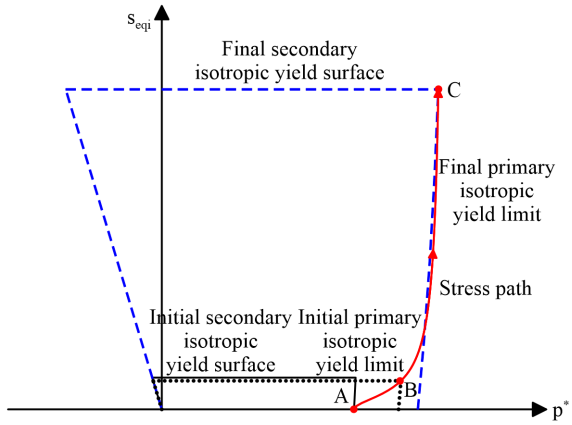

Figure 7. Stress path of freezing for normally consolidated conditions.

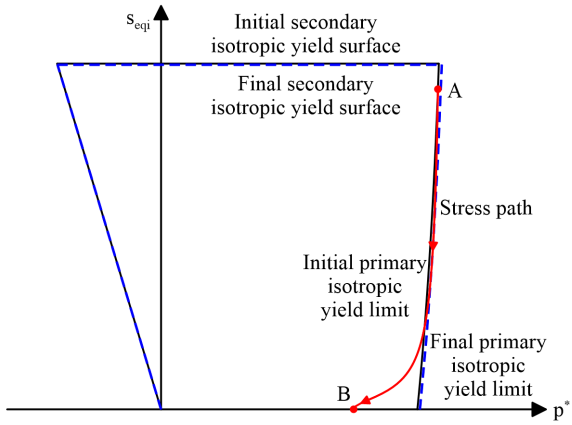

Figure 8. Stress path of thawing for normally consolidated conditions.

4 VERIFICATION

To verify the capability and performance of the proposed model in modelling the constitutive behaviour of fully saturated freezing soils, a series of triaxial tests were simulated. It should be noted that, as existing freezing-thawing tests are performed with a soil column they are essentially boundary value problems, and consequently the relevant simulation needs to account for the complex thermo-hydro-mechanical coupled behaviour of the soil. For this reason, such tests are not considered here.

4.1 *Triaxial tests on fully saturated freezing soils under different temperatures*

A series of triaxial compression tests on fully saturated freezing sand were reported by Xu (2014). These tests were conducted on cylindrical specimens with a diameter of 61.8 mm and a height of 128.0 mm. Rapid freezing at -30 °C was first performed to inhibit the development of freezing fronts and ice lenses. Then, the specimens were heated to the target temperature and subjected to triaxial compression with a constant loading rate of 1.25 mm/min.

The first set of triaxial compression tests were conducted under a constant confining pressure of 1 MPa, with controlled temperatures of -1, -2, -5 and -10 °C. An initial void ratio of 0.4 is considered in the tests. The model parameters employed in the model predictions are summarised in Table 1, with the

associated variation of degree of liquid ice saturation with temperature shown in Figure 9. Figure 10 shows the comparison between model predictions and experimental results, yielding a satisfactory agreement in both $\varepsilon_1 - J^*$ and $\varepsilon_1 - \varepsilon_v$.

Table 1. Values of model parameters for simulation of triaxial tests on freezing sands under various temperatures.

Parameters	Value	Parameters	Value
α_f, μ_f	0.4, 0.5	G_0 (MPa)	3.5
α_g, μ_g	0.8, 0.99	$G_{f_{ref}}$ (MPa)	76.3
M_f, M_g	1.72, 1.52	$G_{f_{inc}}$ (MPa)	20.5
p^c (MPa)	1.0	k	0.15
$\lambda(0)$	0.85	p_{atm} (MPa)	0.1
r	0.67	T_{entry} (°C)	0.0
β (MPa^{-1})	0.1	K_{min} (MPa)	1.0
κ_s	0.008	s_{oi} (MPa)	15.0
υ_1	8.57	λ_s	0.4
p_0^* (MPa)	5.55	ρ_i (t/m^3)	0.9
T_{ref} (K)	-273.16	L_i (kJ/kg)	334.0
κ_0	0.026	s_{l0} (%)	5.0
m_{K_f}	1.1	α	5.0
n_{K_f}	0.75	n	2.0
$T_{E,ref}$ (°C)	0.0	m	0.4

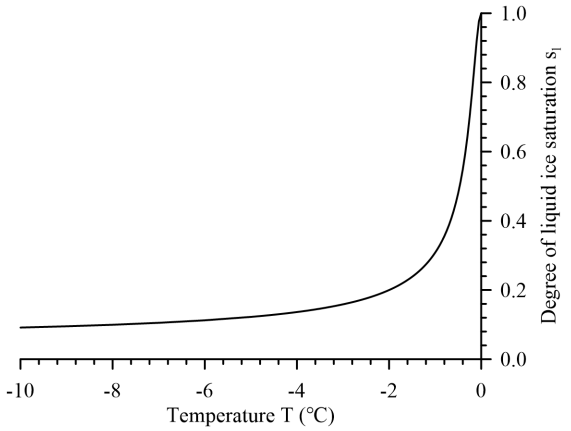

Figure 9. Variation of degree of liquid ice saturation with temperature.

4.2 *Triaxial tests on fully saturated freezing soils under different confining pressures*

Another set of triaxial compression tests were conducted under a constant temperature of -6 °C by Xu (2014), with confining pressures of 0.3, 0.6, 0.8 and 1 MPa. The initial void ratio of 0.3 is considered in the tests. The model parameters employed in the simulations are summarised in Table 2 while the comparison between model predictions and experimental results are shown in Figure 11.

The proposed model was verified to be capable of capturing the behaviour of fully saturated freezing sand under various confining pressures. However, the model predictions were observed to overestimate volumetric strain and the peak strength, which may be caused by the overly large elastic region defined on the dry side of the yield surface. This can be improved by replacing the yield surface on the dry side by the Hvorslev surface (Tsiampousi et al., 2009, 2013).

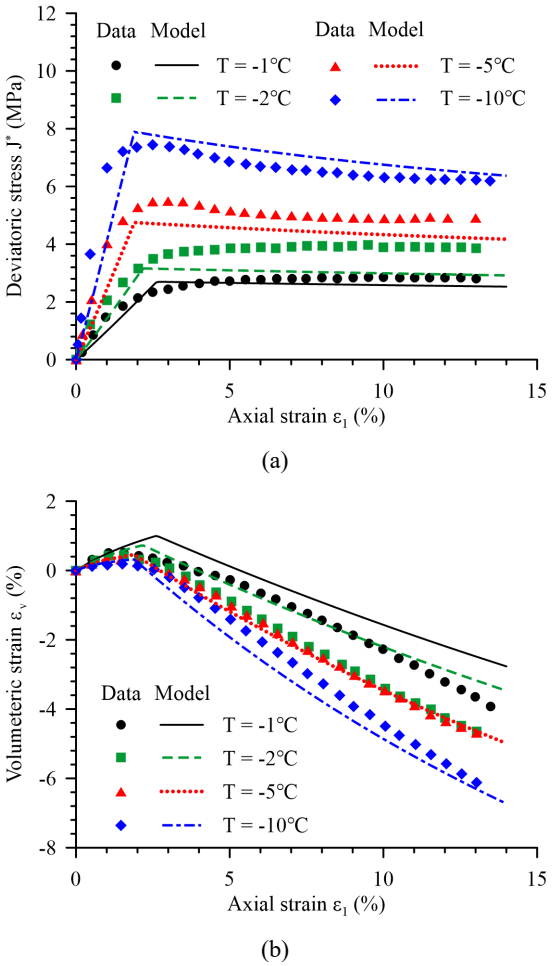

Figure 10. Comparison between model predictions and experimental results for triaxial tests on freezing sands under various temperatures: (a) $\varepsilon_1 - J^*$; (b) $\varepsilon_1 - \varepsilon_v$.

Table 2. Values of model parameters for simulation of triaxial tests on freezing sands under various confining pressures.

Parameters	Value	Parameters	Value
α_f, μ_f	0.5, 0.9	G_0 (MPa)	4.2
α_g, μ_g	0.5, 0.9	$G_{f_{ref}}$ (MPa)	9.1
M_f, M_g	1.2, 1.2	$G_{f_{inc}}$ (MPa)	3.0
p^c (MPa)	0.47	k	0.09
$\lambda(0)$	0.2	p_{atm} (MPa)	0.1
r	0.55	T_{entry} (°C)	0.0
β (MPa^{-1})	0.1	K_{min} (MPa)	1.0
κ_s	0.008	s_{oi} (MPa)	15.0
υ_1	2.74	λ_s	0.4
p_0^* (MPa)	4.2	ρ_i (t/m^3)	0.9
T_{ref} (K)	-273.16	L_i (kJ/kg)	334.0
κ_0	0.038	s_{l0} (%)	5.0
m_{K_f}	0.9	α	5.0
n_{K_f}	0.6	n	2.0
$T_{E,ref}$ (°C)	0.0	m	0.4

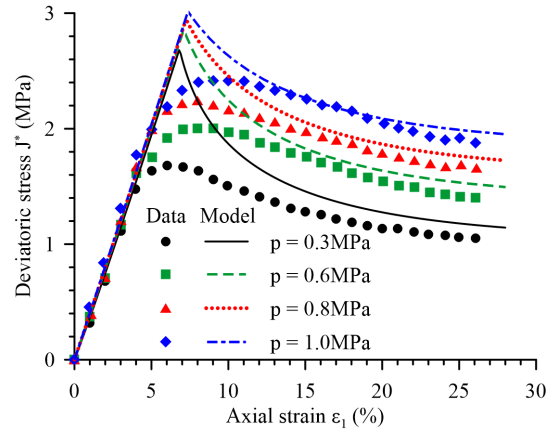

(a)

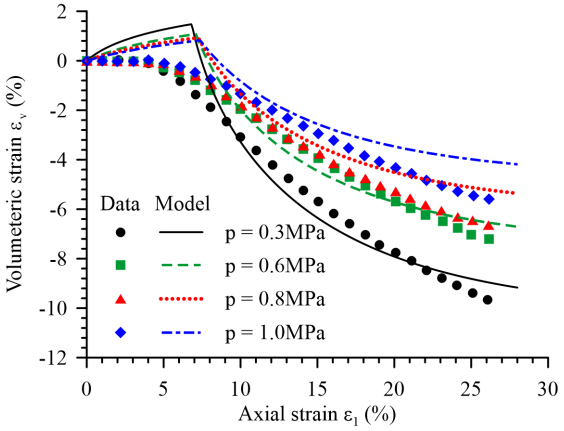

(b)

Figure 11. Comparison between model predictions and experimental results for triaxial tests on freezing sands under different confining pressures: (a) $\varepsilon_1 - \boldsymbol{J}^*$; (b) $\varepsilon_1 - \varepsilon_v$.

5 CONCLUSIONS

This paper presents the development of a constitutive model for fully saturated freezing soils within the framework of double stress variables, in which the solid phase stress and cryogenic suction are adopted as the two independent stress variables. The models behaviour under a freezing-thawing stress path is demonstrated, and its capability is verified against a series of triaxial tests on fully saturated freezing soils. The main conclusions can be summarised as follows:

1. A novel formulation is introduced to adequately model the temperature-dependent variation of elastic bulk and shear moduli for freezing soils. The proposed formulation is shown to overcome the limitation in some existing models in which the elastic moduli cannot reduce to those for a conventional critical state model when the temperature exceeds the freezing point.
2. The characteristics of freezing soils under a freezing-thawing stress path become more complex due to the definition of solid phase stress. A significant difference is found between the proposed model and existing models for partially saturated soils developed within the framework of double stress variables.
3. The proposed model is verified against a series of triaxial compression tests on freezing soils with various temperatures and confining pressures, yielding a good agreement between model predictions and experimental results.
4. To further verify the capability of the proposed model, more advanced laboratory tests for freezing soils, in particular these under complex stress paths, are required in the future.

6 ACKNOWLEDGEMENTS

This work is funded by the National Natural Science Foundation of China (Grant Nos. 52479092 and 52238007).

7 REFERENCES

Alonso, E.E., Gens, A., and Josa A. 1990. A constitutive model for partially saturated soils. *Geotechnique* 40(3), 405-430.

Arenson, L.U., and Springman, S.M. 2005. Mathematical descriptions for the behaviour of ice-rich frozen soils at temperatures close to 0 °C. *Canadian Geotechnical Journal* 42, 431-442.

Black, P.B., and Tice, A.R. 1989. Comparison of soil freezing curve and soil water curve data for windsor sandy loam. *Water Resources Research* 25(10), 2205-2210.

Ghoreishian Amiri, S.A., Grimstad, G., Kadivar, M., and Nordal, S. 2016. Constitutive model for rate-independent behavior of saturated frozen soils. *Canadian Geotechnical Journal* 53, 1646-1657.

Georgiadis, K., Potts, D.M., and Zdravković, L. 2005. Three-dimensional constitutive model for partially and fully saturated soils. *International Journal of Geomechanics* 5, 244-255.

He, P., Zhu, Y., and Cheng, G. 2000. Constitutive models of frozen soil. *Canadian Geotechnical Journal* 37, 811-816.

Lagioia, R., Puzrin, A.M., and Potts, D.M. 1996. A new versatile expression for yield and plastic potential surfaces. *Computers and Geotechnics* 19(3), 171-191.

Lai, Y., Xu, X., Yu, W., and Qi, J. 2014. An experimental investigation of the mechanical behavior and a hyperplastic constitutive model of frozen loess. *International Journal of Engineering Science* 84, 29-53.

Li, N., Chen, F., Xu, B., and Swoboda, G. 2008. Theoretical modeling framework for an unsaturated freezing soil. *Cold Regions Science and Technology* 54, 19-35.

Nicolsky, D.J., Romanovsky, V.E., Tipenko, G.S., and Walker, D.A. 2008. Modeling biogeophysical interactions in nonsorted circles in the Low Arctic. *Journal of Geophysical Research: Biogeosciences* 113(G3), G03S05.

Nishimura, S., Gens, A., Olivella, S., and Jardine, R.J. 2009. THM-coupled finite element analysis of frozen soil: formulation and application. *Geotechnique* 59(3), 159-171.

Nixon, J.F. 1991. Discrete ice lens theory for frost heave in soils. *Canadian Geotechnical Journal* 28(6), 843-859.

Potts, D.M., and Zdravković, L. 1999. *Finite element analysis in geotechnical engineering: Theory*. London: Thomas Telford.

Potts, D.M., and Zdravković, L. 2001. *Finite element analysis in geotechnical engineering: Application*. London: Thomas Telford.

Rostami, H., Ghoreishian Amiri, S.A., and Grimstad, G. 2017. Back analysis of Caen's test by the recently developed frozen/unfrozen soil. *Plaxis Bulletin* 41, 12-19.

Thomas, H.R., Cleall, P., Li, Y.C., Harris, C., and Kern-Luetschg, M. 2009. Modelling of cryogenic processes in permafrost and seasonally frozen soils. *Geotechnique* 59(3), 173-184.

Tsiampousi, A., Zdravković, L. and Potts, D.M. 2009. Modelling of overconsolidated unsaturated soils. *Proc. 4th Asia Pacific conference on unsaturated soils*, Newcastle, Australia, 673-678.

Tsiampousi, A., Zdravković, L. and Potts, D.M. 2013. A new Hvorslev surface for critical state type unsaturated and saturated constitutive models. *Geotechnique* 48, 156-166.

Xu, G. 2014. *Hypoplastic constitutive models for frozen soil*. PhD thesis, University of Natural Resources and Life Sciences, Vienna, Austria.